We are IntechOpen, the world's leading publisher of Open Access books Built by scientists, for scientists

4,800
Open access books available

122,000
International authors and editors

135M
Downloads

Our authors are among the

154
Countries delivered to

TOP 1%
most cited scientists

12.2%
Contributors from top 500 universities

WEB OF SCIENCE™

Selection of our books indexed in the Book Citation Index in Web of Science™ Core Collection (BKCI)

Interested in publishing with us?
Contact book.department@intechopen.com

Numbers displayed above are based on latest data collected.
For more information visit www.intechopen.com

1

Information-Theoretic Modeling and Analysis of Stochastic Behaviors in Quantum-Dot Cellular Automata

Lei Wang[1], Faquir Jain[2] and Fabrizio Lombardi[3]
[1,2]*University of Connecticut*
[3]*Northeastern University*
USA

1. Introduction

Over the last two decades , quantum-dot cellular automata (QCA) has received significant attention as an emerging computing technology (Lent et al., 1993). The basic elements in this technology are the QCA cells, as shown in Fig. 1. Each cell contains two mobile electrons and four quantum dots located in the corners. As per the occupancy of the electrons in the dots, a QCA cell can take different states. A null state (polarization 0) occurs when the electrons are not settled. The other two states are referred to as polarization $+1$ and -1, denoted as $P = +1$ and $P = -1$ respectively. In these states due to Coulombic interactions, the electrons occupy the two diagonal configurations as shown in Fig. 1(b) and (c). These two states are identified with the so-called ground (stable) states. Any intermediate polarization between $+1$ and -1 is defined as a combination of states $P = +1$ and $P = -1$. By encoding the polarizations -1 and $+1$ into binary logic 0 and logic 1, QCA operation can be mapped into binary functions. For clocking and to allow QCA cells to reach a ground state, an adiabatic four-phased switching scheme has been introduced (Lent & Tougaw, 1997). By modulating the tunneling energy between the dots in a cell, this clocking scheme drives each cell through a depolarized state, a latching state, a hold phase, and then back to the depolarized state, such that the information flow is controlled through the QCA devices.

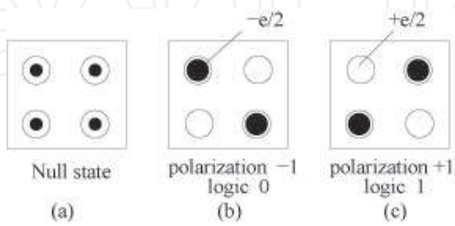

Fig. 1. Schematic of QCA cells: (a) null state, (b) polarization -1, and (c) polarization +1.

Different fabrication technologies (Amlani et al., 1998)–(Jiao et al., 2003) have been proposed to implement QCA devices; QCA logic circuits have also been extensively reported in the literature (Ottavi et al., 2006)–(Tougaw & Lent, 1994). As a common challenge spanning all emerging technologies, the stochastic behaviors of QCA devices impose a significant

hurdle to reliable system integration for high performance and scalability. These stochastic behaviors stem from the nondeterministic quantum mechanisms in combination with the large number of defects and variations from fabrication. In particular, it is anticipated that the defect rates of emerging technologies could be several orders of magnitude higher than today's CMOS. Defect characterization of different QCA implementations has been discussed in (Momenzadeh et al., 2005)–(Niemier et al., 2006).

To achieve reliable operation, defect tolerance is a significant concern. Among many possible alternatives, redundancy-based defect tolerance is one of the most effective approaches. By using shorter QCA lines and exploiting the self-latching property of clocked QCA devices, a triple modular redundancy (TMR) with shifted operands has been proposed in (Wei et al., 2005) to design a 1-bit full adder with the same level of fault/defect tolerance as a conventional TMR. In (Fijany & Toomarian, 2001), a defect-tolerant block majority gate has been proposed for the design of various QCA devices. In (Huang et al., 2006)–(Dysart, 2005), tile-based designs were proposed to improve the reliability of QCA devices. All of these techniques employ spatial redundancy for achieving an improvement in reliability.

While effort has been directed towards the improvement of reliability for emerging technologies, current literature has also shown that it is very difficult to deal with defects/variations at device and circuit levels alone. For QCA devices, analysis of reliability is usually performed on a probabilistic basis. A study in (Liu, 2006) has analyzed the robustness with respect to defects and temperature of clocked metallic and molecular QCA circuits. Methods based on statistical mechanics have been proposed in (Wang & Lieberman, 2004) to investigate the total number of QCA cells that could correctly operate together in a molecular QCA device prior to thermal fluctuations (as causing errors at the output). In (Niemier et al., 2006), the probability of a correct output in molecular QCA devices has been established with respect to spacing and cell size by utilizing a statistical quantum mechanical analysis. In (Dysart & Kogge, 2007), probabilistic transfer matrices were employed to study the effectiveness of TMR on the reliability improvement for a 1-bit full adder. A probabilistic model based on Bayesian networks has been proposed in (Bhanja & Sarkar, 2006), (Srivastava & Bhanja, 2007) to model the cell state probabilities of QCA devices for input polarizations. The reliability of QCA devices subject to variations in temperature has been also assessed in (Bhanja et al., 2006), (Ungarelli et al., 2000).

Few results exist in determining the fundamental limit on achievable reliability given the stochastic nature of emerging technologies. In the past, this problem was investigated for conventional logic gates. In (von Neumann, 1955), a multiplexing technique was proposed to obtain reliable synthesis from unreliable components. Since then, several approaches have been reported in deriving the error bounds for individual gates. It was theoretically proved in (Pippenger, 1985), (Pippenger, 1989) that with constant multiplicative redundancy, a variety of Boolean functions built upon unreliable components may be operated reliably. The error bounds were derived for three-input majority gates (Hajek & Weller, 1991), arbitrary-input majority gates (Evans & Schulman, 1999), and two-input NAND gates (Evans & Pippenger, 1998). A nonlinear mapping and bifurcation approach was proposed in (Gao et al., 2005) to provide a new solution to this problem. In (Bhaduri & Shukla, 2005), entropy was used to describe the energy of noisy logic states thereby reflecting the uncertainty inherent in thermodynamics. It should be pointed out that most of these studies were based on the general von Neumann model of basic gate errors, which is more suitable to describe transient errors caused by signal noise in conventional digital logic. The information storage capacity of a

crossbar switching network was derived in (Sotiriadis, 2006). This work, however, does not consider the defects in molecular devices explicitly.

In this chapter, we present an information-theoretic framework to investigate the relationship between stochastic behaviors and achievable reliable performance in QCA technology. The central idea is that QCA devices can be modeled as a network of unreliable information processing channels. In contrast to probabilistic measures at device/circuit levels, this model allows us to employ information-theoretic concepts (Shannon, 1948) and study some fundamental issues associated with the QCA technology. Specifically, we employ an information-theoretic analysis to QCA devices by explicitly considering the quantum mechanisms of this technology. By employing statistical channel models, we derive information-theoretic measures to quantify various nano/molecular effects such as cell displacement and misalignment. We determine the information transfer capacity that, from the information-theoretic viewpoint, can be interpreted as the achievable bound on the reliability for QCA devices. One key problem that we will address is what level of redundancy is needed to achieve reliable operation out of unreliable QCA devices. The proposed method provides us with a common framework to evaluate the effectiveness of redundancy-based defect tolerance in a quantitative manner.

We will review the relevant information-theoretic concepts that provide the basis of this work. We will then discuss various stochastic behaviors in QCA devices and develop an information-theoretic framework for the analysis of reliable operation in the presence of defects and variations. By applying the proposed method, we determine the achievable bound on the reliability of QCA devices.

2. Preliminaries

Emerging technologies such as QCA present a large degree of uncertainty in operation due to the underlying quantum mechanisms; these mechanisms inevitably lead to a large number of defects and variations in the implementation and operation of QCA devices and circuits. Therefore, it is necessary to develop a common framework for evaluating these non-ideal effects and their impact on system-level performance. In this work, we model QCA devices as defect-prone information processing media and employ information-theoretic measures to investigate the reliability problems associated with them. This section will review the information-theoretic concepts relevant to the proposed analysis.

Consider a discrete variable X with alphabet $\mathcal{X}$ and probability distribution function $p(x) \triangleq Pr\{X = x\}$, where $x \in \mathcal{X}$. From Shannon's joint source-channel coding theory (Shannon, 1948), the entropy $H(X)$ of this variable is defined as

$$H(X) \triangleq -\sum_{x \in \mathcal{X}} p(x) \log_2(p(x)), \tag{1}$$

where $H(X)$ is expressed in bits.

The entropy $H(X)$ is a measure of the information content in the variable X. A higher entropy implies a greater uncertainty in this variable and thus, the larger information content it carries. Assume that the variable X is passed through a transformation $\mathcal{F} : X \rightarrow Y$, where $\mathcal{F}$ is a non-ideal (e.g., error-prone) mapping function from $X \in \mathcal{X}$ to $Y \in \mathcal{Y}$. The mutual information $I(X;Y)$ between X and Y is defined as

$$\begin{aligned} I(X;Y) &= H(X) - H(X|Y) \\ &= H(Y) - H(Y|X), \end{aligned} \tag{2}$$

where $H(Y|X)$ is the conditional entropy of Y conditioned on X, and it is expressed as

$$\begin{aligned} H(Y|X) &= -\sum_{x\in\mathcal{X}}\sum_{y\in\mathcal{Y}} p(x,y)\log_2(p(y|x)) \\ &= -\sum_{x\in\mathcal{X}}\sum_{y\in\mathcal{Y}} p(x)p(y|x)\log_2(p(y|x)), \end{aligned} \tag{3}$$

where $p(x,y)$ and $p(y|x)$ are the joint probability and conditional probability, respectively, of variables X and Y. For a given $\mathcal{F}$, the values of $p(x,y)$ and $p(y|x)$ are determined by the distribution of the input X.

The conditional entropy $H(Y|X)$ can be viewed as the residual uncertainty in Y given the knowledge of X. Thus, the mutual information $I(X;Y)$ measures the reduction in uncertainty in Y (by an amount $H(Y|X)$) due to the information transferred through $\mathcal{F}$.

The maximum information content that can be transferred through the transformation $\mathcal{F}$ with an arbitrarily low error probability, is given by its capacity as

$$C_u = \max_{\forall p(x)} I(X;Y), \tag{4}$$

where C_u is the information transfer capacity per use obtained by maximizing over all possible distributions of the input X.

The information transfer capacity C_u represents the achievable bound on the reliable operation in a non-ideal information processing medium. The following example illustrates these information-theoretic measures as applied to a conventional CMOS gate.

Example 1: Consider a 2-input NAND gate in conventional CMOS technology. Assume that the implementation of this gate is non-ideal such that the output will generate errors (e.g., due to variations of process parameters, voltage and temperature) at a probability $\varepsilon = 10^{-6}$. By employing (1)−(3), the information transfer capacity of this error-prone gate can be obtained as

$$\begin{aligned} C_u &= \max_{\forall p(x)}\{H(Y) - H(Y|X)\} \\ &= 1 + \varepsilon\log_2\varepsilon + (1-\varepsilon)\log_2(1-\varepsilon) \\ &= 0.99997 \text{ bits/use}. \end{aligned} \tag{5}$$

As indicated, the information transfer capacity is very close to 1 bit per use. Note that an ideal error-free NAND gate is able to transfer at most 1 bit of information per use; thus for an error rate as low as 10^{-6}, this gate is quite reliable.

Figure 2 compares the information transfer capacity under different error rates. The information transfer capacity of the NAND gate is symmetric around an error rate of 0.5. This indicates that from an information-theoretic viewpoint, the NAND gate is able to achieve the same level of reliability under a pair of error rates ε_1 and $\varepsilon_2 = 1 - \varepsilon_1$. This is not surprising because for an error rate larger than 0.5, we can deliberately interpret the output by its complement as the gate actually produces more errors than correct results.

Note that the above example concerns transient output errors, of which the error rate is typically obtained by averaging over time (Wang & Shanbhag, 2003). In emerging technologies, defects from fabrication have become a critical problem. The defect rate p_d reflects the spatial variations over different fabricated samples. Thus, although defects are permanent in a given sample, the nature of randomness stands when considering a large number of samples. In other words, the occurrence and location of defects vary with great uncertainty across these samples. Without conducting an exhaustive test, one can only say

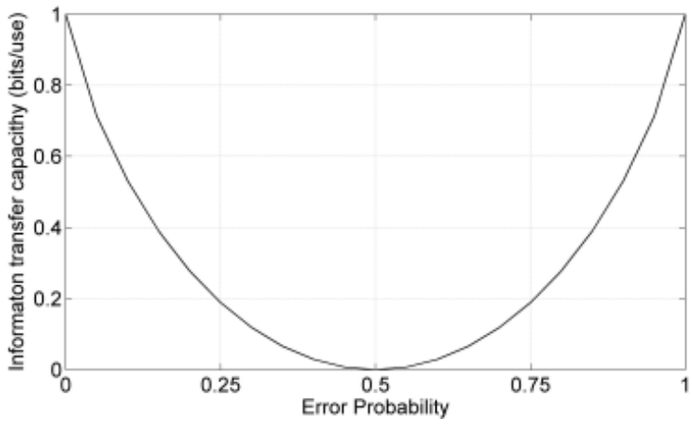

Fig. 2. Information transfer capacity of a NAND gate under different error rates.

that a circuit may be defective with a probability of p_d. The following example illustrates the information-theoretic measures for nanowire crossbars under this scenario.

Example 2: Consider a 2-input AND gate implemented by two different nanowire crossbar columns, one with 2 crosspoints and the other providing 3 crosspoints where one crosspoint is redundant. In both cases the defect rate is assumed to be $p_d = 0.1$.

Case 1: In this case, a 2-crosspoint column is employed to implement the 2-input AND gate. Note that this implementation does not provide any redundancy. It can be shown (Dai et al., 2009) that the conditional probability of the output Y conditioned on the input X is

$$\begin{aligned} &P(Y=1|X=00)=0.01,\\ &P(Y=1|X=01)=0.09,\\ &P(Y=1|X=10)=0.09,\\ &P(Y=1|X=11)=1,\\ &P(Y=0|X)=1-P(Y=1|X). \end{aligned} \tag{6}$$

Substituting these values into (1)−(3), we obtain $C_u = 0.959$ bits/use. Comparing this result with the Example 1, the achievable bound on reliability as measured by C_u is reduced due to the high defect rate in nanowire crossbars.

Case 2: The second case introduces one redundant crosspoint in implementing the 2-input AND gate. Applying the method in (Dai et al., 2009), we get

$$\begin{aligned} &P(Y=1|X=00)=0.001,\\ &P(Y=1|X=01)=0.0145,\\ &P(Y=1|X=10)=0.0145,\\ &P(Y=1|X=11)=1,\\ &P(Y=0|X)=1-P(Y=1|X), \end{aligned} \tag{7}$$

and proceeding in the same way, we obtain $C_u = 0.994$ bits/use.

Apparently, the bound on reliability is improved by exploiting the redundancy in nanowire crossbars. Information-theoretic measures enable us to quantify this improvement and thus evaluate the effectiveness of redundancy-based defect tolerance in an analytical manner. Questions arise on how much redundancy is needed in order to obtain a desired level of

reliable performance. Naturally, we would also like to compare the achievable reliability of OCA devices with conventional CMOS technology. These problems will be addressed in the following sections.

3. Information-theoretic analysis of QCA

In this section, we will show that the stochastic behaviors of QCA enable us to model these devices as unreliable information processing channels. While different QCA implementations (Amlani et al., 1998)–(Jiao et al., 2003) have been proposed, we will focus on lithographically made QCA devices which are electrostatic based. We will first discuss the possible defects in QCA technology and then develop statistical channel models for various QCA devices. Based on these models, we will derive the information-theoretic measures to quantify the uncertainties in the operation of QCA devices.

3.1 Defects in QCA

Under their manufacturing process, lithographically made QCA devices are likely to have defects. It has been reported that defects can occur in both the synthesis and the deposition phases (Momenzadeh et al., 2005), (Taboori et al., 2004) of QCA devices. In the synthesis phase, a cell may have missing or extra (additional) dots and/or electrons, while in the deposition phase cell misplacement may occur. It has been projected that defects caused by cell misplacement will be dominant in QCA devices due to the difficulty in precise control of the cell location at nanoscale ranges. The various types of cell misplacement that may occur, are as follows:

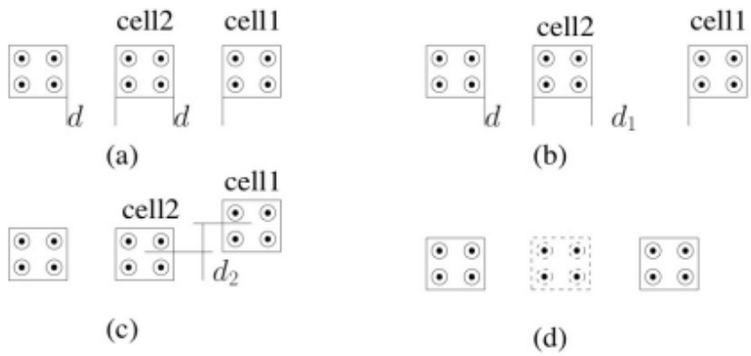

Fig. 3. Three types of misplacement: (a) defect-free, (b) displacement, (c) misalignment, and (d) omission.

1.) *Cell displacement* represents a type of defect in which the distance between cells does not match the nominal value. As shown in Fig. 3(b), the distance between cell1 and cell2 should be equal to d in the correct (ideal) design. Due to displacement, the distance becomes d_1 in the fabricated device.
2.) *Cell misalignment* indicates the deviation in cell location along certain directions. As shown in Fig. 3(c), cell1 has a vertical misalignment equal to d_2, whereas in the ideal case this value should be zero.
3.) *Cell omission* occurs when a particular cell is missing from its pre-specified location in the layout. This is shown in Fig. 3(d). Cell omission may not be a dominant type of defects in lithographically made QCA devices.

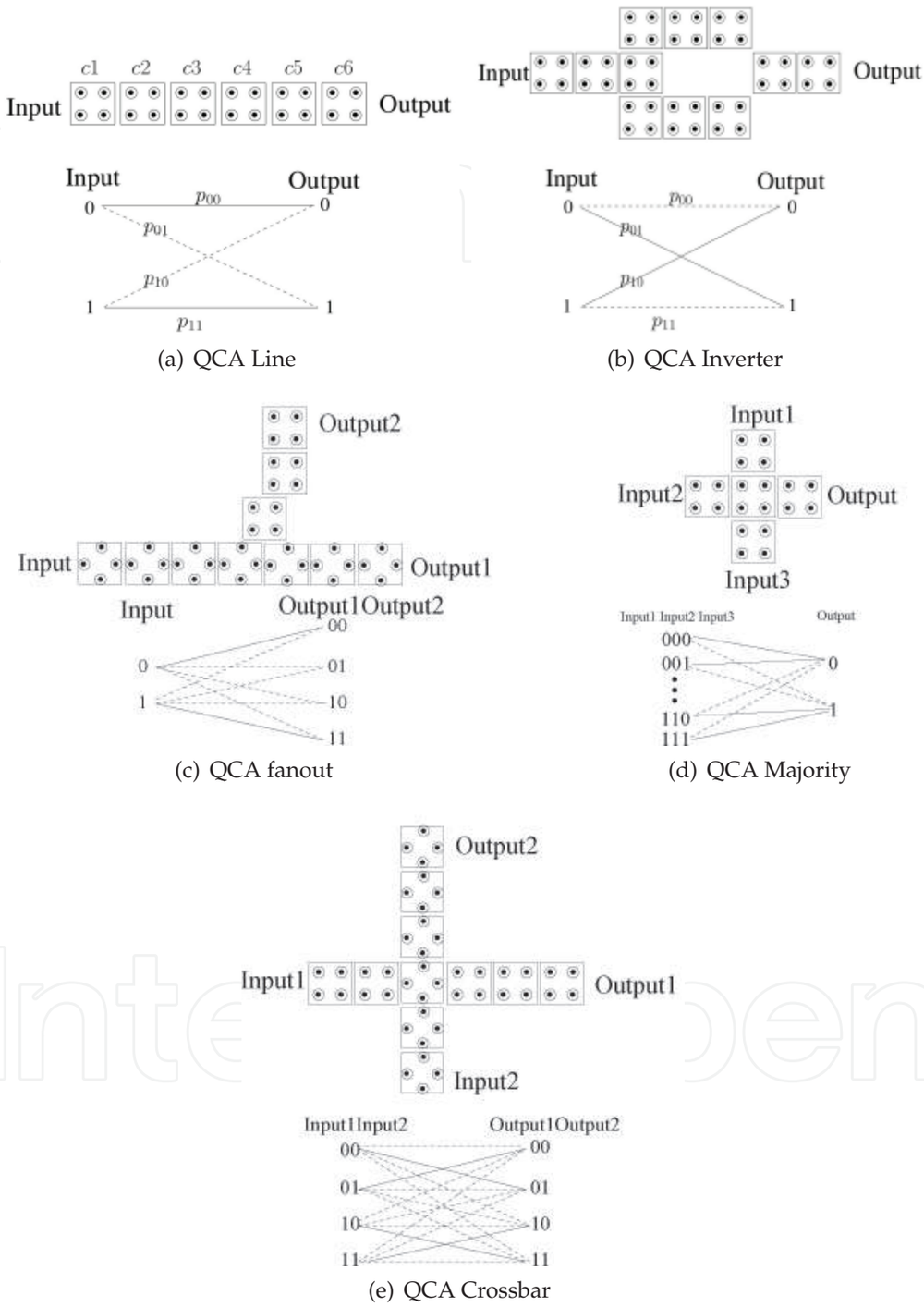

(a) QCA Line (b) QCA Inverter

(c) QCA fanout (d) QCA Majority

(e) QCA Crossbar

Fig. 4. Statistical channel models for different QCA devices.

In addition to the above defects, device size and temperature will also affect the operation of QCA devices. As shown in the following section, these factors affect the density matrices and thus the values of statistical mapping p_{ij} in the channel model (refer to Fig. 4). This in turn will affect the values of the information-theoretic measures such as channel capacity.

3.2 Statistical channel models of QCA devices

For an error-free logic function, the mapping between the input and output is well-defined, i.e., $P(Y = y_o|X = x_i) \equiv 1$, where $X = x_i$ is the input and $Y = y_o$ is the corresponding output determined by the logic function. However, QCA devices are nondeterministic because each input will only generate an output with certain probability. This phenomenon is further complicated by the presence of defects as discussed previously in section 3.1. Therefore, mappings between the input and output of QCA devices may not follow predefined functions. These uncertainties can be modeled by employing statistical information processing channels, as illustrated in Fig. 4 for QCA devices. In these models, the unreliable logic operation is quantified by the probability $p_{ij} = p(Y_j|X_i)$, i.e., the probability of the output $Y = Y_j$ conditioned on the input $X = X_i$. The solid lines in these models indicate the desired mappings (e.g., the correct output determined by the logic function), whereas the dotted lines represent the erroneous mappings induced by defects and variations.

For QCA, the desired output is generated with certain probability even when the implementation is perfect. Therefore, the p_{ij}'s of the desired mappings are not equal to 1 in the general case. For erroneous mappings the p_{ij}'s are also a function of defects and variations. By employing the statistical channel models, we can assess the impact of these stochastic behaviors using information-theoretic measures, as discussed in the next subsection.

The proposed statistical channel models can also be applied to assess other features of QCA. Different QCA implementations are affected by different types of defects and fabrication variations. This diversity may result in changes of topology (e.g., when the entire parts of a circuit are missing) or numerical values of the mapping p_{ij} (e.g., when defects/variations have different statistics) in the corresponding channel model in Fig. 4. However, the information-theoretic measures and the relationship between defects/variations and performance can be determined in the same manner using the proposed method, thus showing its flexibility in various applications.

3.3 Information transfer capacity of QCA devices

We now derive the information-theoretic measures for investigating the uncertainties in the computing process performed by unreliable QCA devices. As clocking schemes for QCA are typically implemented in a relatively reliable technology such as CMOS (Momenzadeh et al., 2005), (Hennessy & Lent, 2001), (Niemier et al., 2007), we assume these schemes to be highly reliable relative to QCA; thus only defects/variations related to QCA devices and circuits (which operate under an adiabatic four-phased clocking scheme) are considered in the following analysis.

From section 2, to derive information-theoretic measures such as entropy and information transfer capacity, the conditional probabilities p_{ij}'s between the input and output of QCA devices (modeled by the statistical channels in Fig. 4) must be established. These conditional probabilities can be determined by examining the underlying quantum mechanisms of QCA. Unlike conventional CMOS in which computation is performed by voltage/current levels, QCA operates through Coulombic interactions among neighboring cells by affecting their polarizations. The Coulombic interaction between any two cells can be characterized by the

so-called kink energy E_k. Let $E^{i,j}_{opposite}$ and $E^{i,j}_{same}$ denote the energy between two cells i and j with opposite polarization and with same polarization, respectively. The kink energy between these two cells can be expressed as

$$E^{i,j}_k = E^{i,j}_{opposite} - E^{i,j}_{same}, \tag{8}$$

and $E^{i,j}_{opposite}$ and $E^{i,j}_{same}$ can be calculated from

$$E^{i,j} = \frac{1}{4\pi\varepsilon_0\varepsilon_r} \sum_{n=1}^{4} \sum_{m=1}^{4} \frac{q^i_n q^j_m}{|r^i_n - r^j_m|}, \tag{9}$$

where ε_0 is the permittivity of free space, ε_r is the dielectric constant, q^i_n and q^j_m are the charges in dot n of cell i and dot m of cell j, respectively. The positions of dot n of cell i and dot m of cell j are denoted by r^i_n and r^j_m, respectively. From (9), the kink energy between cells i and j depends on their relative locations.

By employing the kink energy, the matrix representation of the Hamiltonian using the Hartree-Fock approximation is given by (Timler & Lent, 2002)

$$H = \begin{bmatrix} -\frac{1}{2}\sum_{j\in\Omega_i} E^{i,j}_k P_j & -\gamma_i \\ -\gamma_i & \frac{1}{2}\sum_{j\in\Omega_i} E^{i,j}_k P_j \end{bmatrix}, \tag{10}$$

where $E^{i,j}_k$ is given by (8), Ω_i represents the set of neighboring cells of cell i within the so-called "radius of effect", P_j indicates the polarization of the j^{th} neighboring cell, and γ_i is the tunneling energy between the two states of cell i.

From (Timler & Lent, 1996), (Mahler & Weberrruss, 1998), QCA cells tend to settle to the ground states due to inelastic dissipative heat bath coupling. When QCA cells achieve thermal equilibrium, the steady-state density matrix can be derived from (10) as

$$\rho^{ss} = \frac{e^{-H/KT}}{\mathrm{Tr}[e^{-H/KT}]}, \tag{11}$$

where H is defined in (10), K is Boltzmann constant, and T is the operating temperature. Using the diagonal entries ρ^{ss}_{11} and ρ^{ss}_{00} of this density matrix, we can get the steady-state polarization of cell i as

$$P^{ss}_i = \rho^{ss}_{11} - \rho^{ss}_{00} = \frac{E}{\Lambda}\tanh(\Delta), \tag{12}$$

where

$$E = \frac{1}{2}\sum_{j\in\Omega_i} E^{i,j}_k P_j, \tag{13}$$

$$\Lambda = \sqrt{E^2/4 + \gamma_i^2}, \tag{14}$$

$$\Delta = \frac{\Lambda}{KT}. \tag{15}$$

Applying a self-consistent approximation by factorizing the joint wave function over all cells into a product of individual cell wave functions, the polarization of the output cells can be

determined under a specific polarization (as applied to the input cells). Let P_{ij}^{ss} denote the polarization of the i^{th} output cell under the given polarization of a set (indexed by j) of neighboring cells (e.g., cells in Ω_i as in (10)). These neighboring cells can be considered as the inputs of the i^{th} output cell, so the conditional probabilities with respect to the logic value corresponding to the polarization between the set of input cells $\{x_j\}$ and the output cell y_i can be obtained as (Bhanja & Sarkar, 2006)

$$P(y_i = 1|\{x_j\}) = 0.5(1 + P_{ij}^{ss}), \tag{16}$$

$$P(y_i = 0|\{x_j\}) = 0.5(1 - P_{ij}^{ss}), \tag{17}$$

where P_{ij}^{ss} is given by (12) with the set of input cells $\{x_j\}$ expressed explicitly. The above expressions on conditional probabilities can also be applied to the case in which the input cells themselves are out of the radius of effect of the output cells, however they are connected to the output cells via some intermediate cells. In this case, the polarization of the primary input cells will affect their neighboring cells which in turn will affect the final output cells. Thus, the value of P_{ij}^{ss} is determined iteratively from the primary input cells to the final output cell. In section 4, a design tool QCADesigner (Walus et al., 2004) is employed to compute P_{ij}^{ss} for various QCA devices. Note that we do not make any assumption on the polarization of neighboring cells when deriving (16) and (17).

Based on the conditional probabilities in (16) and (17), the information-theoretic measures (such as output entropy and mutual information for a generic QCA circuit) can be derived as

$$\begin{aligned} H(Y) = &- \sum_{Y_i \in \mathcal{Y}} \Big(\sum_{X_j \in \mathcal{X}} 0.5^L \prod_{\substack{y_m \in Y_i y_n \in Y_i \\ y_m = 1 \; y_n = 0}} (1 + P_{mp,X_j}^{ss})(1 - P_{nr,X_j}^{ss}) \Big) \\ &\times \log_2 \Big(\sum_{X_j \in \mathcal{X}} 0.5^L \prod_{\substack{y_m \in Y_i y_n \in Y_i \\ y_m = 1 \; y_n = 0}} (1 + P_{mp,X_j}^{ss})(1 - P_{nr,X_j}^{ss}) \Big), \end{aligned} \tag{18}$$

$$\begin{aligned} &H(Y|X) = \\ &- \sum_{X_j \in \mathcal{X}} \sum_{Y_i \in \mathcal{Y}} p(X = X_j) \times 0.5^L \prod_{\substack{y_m \in Y_i y_n \in Y_i \\ y_m = 1 \; y_n = 0}} (1 + P_{mp,X_j}^{ss}) \\ &(1 - P_{nr,X_j}^{ss}) \times \log_2 (0.5^L \prod_{\substack{y_m \in Y_i y_n \in Y_i \\ y_m = 1 \; y_n = 0}} (1 + P_{mp,X_j}^{ss})(1 - P_{nr,X_j}^{ss})), \end{aligned} \tag{19}$$

where $X_j \in \mathcal{X}$ is the primary input, $Y_i \in \mathcal{Y}$ is the final output, y_m and y_n are the 1-value and 0-value bits, respectively, of Y_i, P_{mp,X_j}^{ss} and P_{nr,X_j}^{ss} are the polarizations of the output cells y_m and y_n with neighboring cells x_p and x_r, respectively, under a specific input X_j.

The information transfer capacity of the QCA circuit can be determined accordingly as

$$C_u = \max_{\forall p(x)} (H(Y) - H(Y|X)), \tag{20}$$

where the maximization is taken over all possible inputs under the assumption that independent defects and variations are applicable. This assumption reflects the worst case scenario (i.e. it is pessimistic) because independent defects/variations incur the largest

information loss (Shannon, 1948). Thus, the resulting information transfer capacity will be lower than for correlated defects/variations. Moreover, the information transfer capacity represents the upper bound on reliability that a QCA circuit can achieve.

Using information-theoretic measures, uncertainties in the operation of QCA devices can be studied based on the polarizations provided at the input cells and the topological structure of the QCA devices. A QCA line is used next as an example to illustrate this process.

Example 3: Consider a QCA line as shown in Fig. 4(a), where cells $c1$ and $c6$ are the input and output, respectively. The size of these cells is 20nm, the cell-to-cell pitch is $d = 20$nm, and the radius of effect is assumed to be 80nm. The clocking scheme is not shown as it won't affect our analysis (i.e., it is much more reliable than the QCA line). Initially the polarization of all six cells is in the -1 state. After the polarization $+1$ is applied at the input cell, a multiple iterative process (Walus et al., 2004) is carried out to determine the polarization of all cells in the QCA line, including the output cell $c6$. Initially, $c2$ is taken as the target cell under the new input polarization. Based on the radius of effect, the polarization of $c2$ is calculated under the influence of neighboring cells $c1$, $c3$, $c4$, and $c5$, as indicated by $\Omega_2 = \{c1, c3, c4, c5\}$ in (10) for cell $c2$. Using the relative distances between the dots in $c2$ and the dots in other cells (e.g., $|r_n^i - r_m^j|$ in (9)), the charges q_n^i, q_m^j of each dot in these cells are determined. Substituting these values into (9) and (10), we can determine the values of the kink energy between $c2$ and its neighboring cells $c1$, $c3$, $c4$, and $c5$. From these kink energies and the initial polarizations of the neighboring cells, the matrix representation of the Hamiltonian H can be formed and a new polarization of $c2$ will be determined by solving (11) and (12). This procedure is repeated iteratively for all cells in the QCA line. Once all cells have settled in the stable states, the polarization of the output cell can be obtained for the given input polarization. For this example, the polarization of the output cell $c6$ is found to be 0.95425 when the input $c1$ is $+1$.

Similarly, it is possible to determine the polarization of the output cell under other values of input polarization. Therefore, from (16)$-$(19) we get

$$H(Y) = - \sum_{Y_i \in \{0,1\}} \Big(\sum_{X_j \in \{0,1\}} 0.5 \times S \Big) \times \log_2 \Big(\sum_{X_j \in \{0,1\}} (0.5 \times S) \Big), \tag{21}$$

$$H(Y|X) = - \sum_{X_j \in \{0,1\}} \sum_{Y_i \in \{0,1\}} p(X = X_j) \times 0.5 \times S \times \log_2(0.5 \times S), \tag{22}$$

where

$$S = \begin{cases} (1 + P^{ss}_{1p,X_j}) \text{ for } Y_i = 1,\ X = X_j, \\ (1 - P^{ss}_{1p,X_j}) \text{ for } Y_i = 0,\ X = X_j. \end{cases}$$

Finally, the information transfer capacity of this QCA line can be determined as $C_u = 0.8427$ bits/use. Note that this result is obtained for a defect-free implementation. Compared with the CMOS gate in Example 1 (in which an ideal implementation achieves $C_u = 1$ bit/use), the achievable bound on reliable operation (as measured by the information transfer capacity) is significantly lower in QCA devices. This is not surprising because QCA devices are inherently nondeterministic.

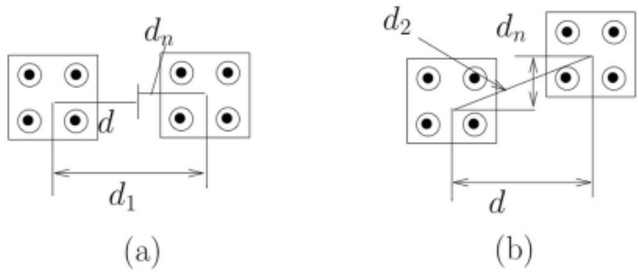

Fig. 5. Defects due to (a) displacement and (b) misalignment.

3.4 Effects of Defects on Information-Theoretic Measures

QCA devices also suffer from a large number of defects and variations in manufacturing and design. Defects can affect the information-theoretic measures as derived previously. Consider a pair of cells such that cell i is defect-free, but cell j is misplaced by an offset η_j from its desired location. The difference in polarization energy between the defect-free and defective implementations can be derived from (9) as follows

$$\begin{aligned}\sigma^{i,j} &= E_f^{i,j} - E_d^{i,j} \\ &= \frac{1}{4\pi\varepsilon_0\varepsilon_r}\sum_{n=1}^{4}\sum_{m=1}^{4} q_n^i q_m^j \left(\frac{1}{|r_n^i - r_m^j|} - \frac{1}{|r_n^i - (r_m^j + \eta^j)|}\right),\end{aligned} \tag{23}$$

where $E_d^{i,j}$ and $E_f^{i,j}$ represent the $E^{i,j}$ for the defective and defect-free cases, respectively.

The presence of $\sigma^{i,j}$ will lead to a different kink energy between the two cells. Let $E_{k,d}^{i,j}$ and $E_{k,f}^{i,j}$ denote the kink energy for the defective and defect-free cases, respectively. Thus,

$$E_{k,d}^{i,j} = E_{k,f}^{i,j} + \delta^{i,j}, \tag{24}$$

where $\delta^{i,j}$ can be obtained from (23) and (8). Substituting $E_{k,d}^{i,j}$ into (10) and (11), the matrix representation of the Hamiltonian can be obtained for cell i. The difference in matrix representation compared to a defect-free device is given by

$$\Delta_H = \begin{bmatrix} -\frac{1}{2}\sum_{j\in\Omega_i}\delta^{i,j}P_j & 0 \\ 0 & \frac{1}{2}\sum_{j\in\Omega_i}\delta^{i,j}P_j \end{bmatrix}. \tag{25}$$

Due to this difference, the steady state matrix ρ^{ss} in (11) and the steady state polarization P_i^{ss} in (12) of cell i are changed by the misplacement in cell j. According to (16) and (17), the conditional probabilities between cells i and j will also be affected which in turn will affect the information-theoretic measures of this QCA circuit.

Figure 5 illustrates two examples of cell misalignment and displacement defects. Assume d is the cell-to-cell pitch in the defect-free case and d_n is the defective misplacement. The actual distances between the two cells are therefore

$$d_1 = d + d_n, \tag{26}$$

$$d_2 = \sqrt{d^2 + d_n^2}. \tag{27}$$

The cell misalignment and displacement defects will have a different impact on the information-theoretic measures of QCA devices. In the next section, we will show the application of the proposed method when analyzing these defects.

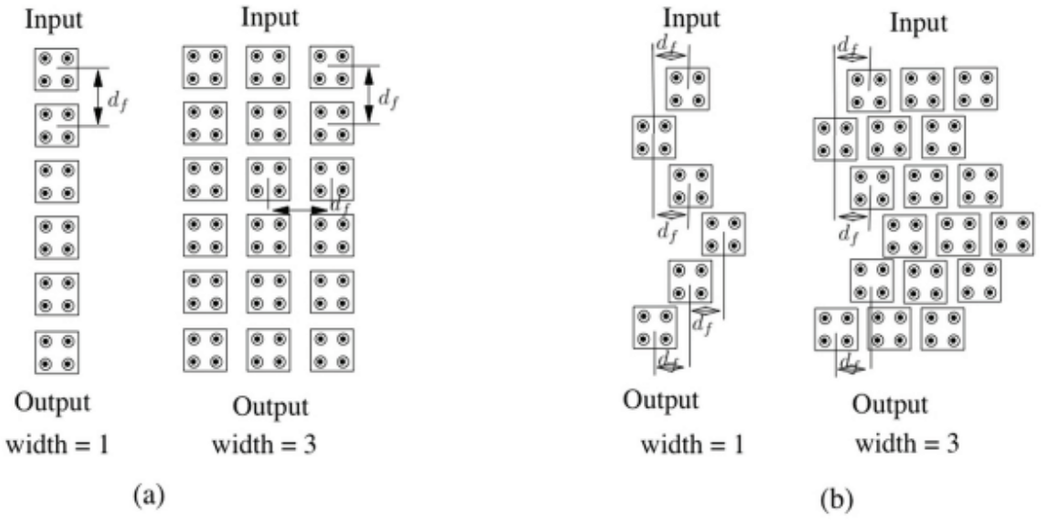

Fig. 6. Tile-based design of a QCA line under (a) displacement (b) misalignment defects.

4. Evaluation and discussion

Tile-based QCA design employs spatial redundancy to overcome various defects and variations in QCA devices (Huang et al., 2006)–(Dysart, 2005). It is a modular approach based on elementary building blocks to construct QCA circuits. The building blocks are referred to as tiles. The width of a tile can be adjusted to achieve different levels of reliability. In this section, we will study the effectiveness of this technique by using the proposed information-theoretic measures. We will consider cell displacement and misalignment defects. The coherence vector simulation engine QCADesigner v2.0.3 (Walus et al., 2004) is utilized to obtain an accurate result on the polarization. The parameters used in the simulation are as follows: cell dimension 18nm, cell-to-cell pitch 20nm, radius of effect 80nm, relative permittivity 12.9. Lithographically made QCA devices require a very low temperature (few degrees Kelvin). Therefore in the simulation, a temperature of 1K is chosen; this is consistent with many existing works (Srivastava & Bhanja, 2007), (Schulhof et al., 2007). An adiabatic four-phased clocking scheme is employed in the QCA circuits.

The QCA devices in Fig. 4 are evaluated under cell displacement defects first. QCA lines with widths of 1 and 3 (shown in Fig. 6(a)) are utilized for the simulation setup. For each simulation run, the same cell displacement d_f is applied to all cell-to-cell pitches. As discussed in section 3.4, cell displacements affect the inter-cell quantum mechanisms and the P_{ij}^{ss} in (16) and (17), thus changing the information transfer capacity.

Figure 7 shows the information transfer capacity of different QCA devices implemented by different widths (e.g., levels of spatial redundancy) subject to displacements from 0% to 30% of the size of the QCA cells. As reported in (Timler & Lent, 1996), a displacement of 30% of cell size is sufficient to affect the correct operation of a QCA device. For QCA crossbars, only the width of horizontal lines is increased (as proposed in (Bhanja et al., 2006)). Some important phenomena are observed from the simulation results. The information transfer capacity of

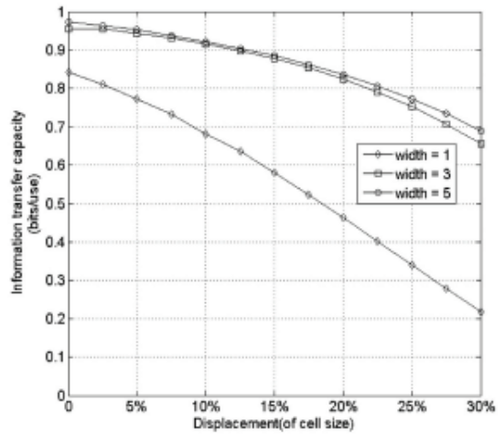

(a) QCA Line

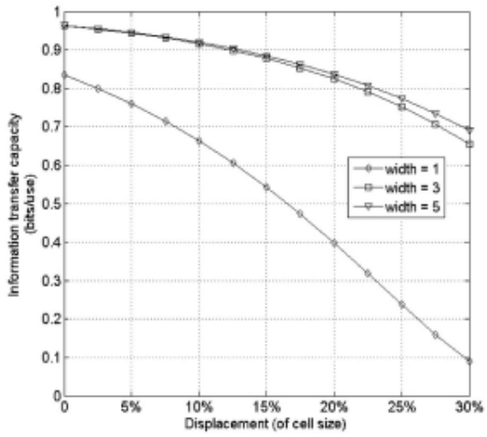

(b) QCA Inverter

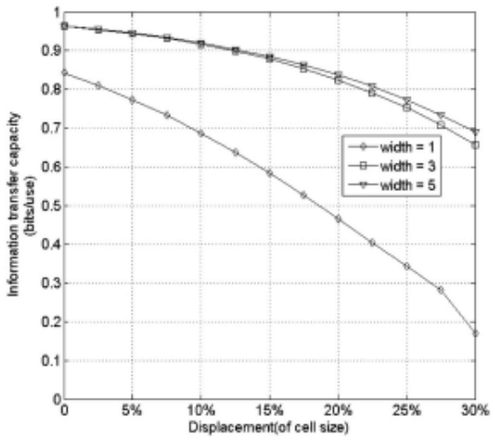

(c) QCA Majority

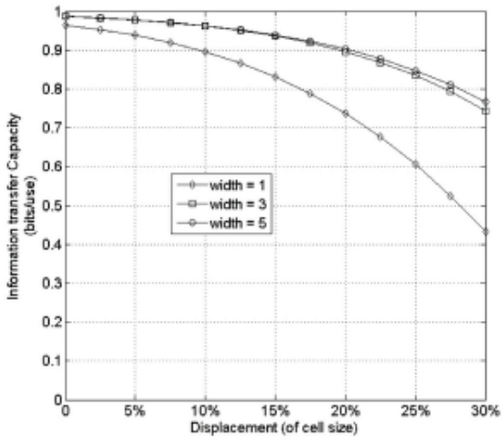

(d) QCA Crossbar

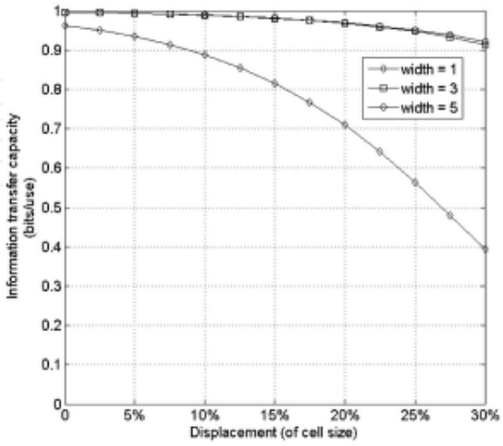

(e) QCA Fanout

Fig. 7. Information transfer capacity of QCA devices under cell displacement defects.

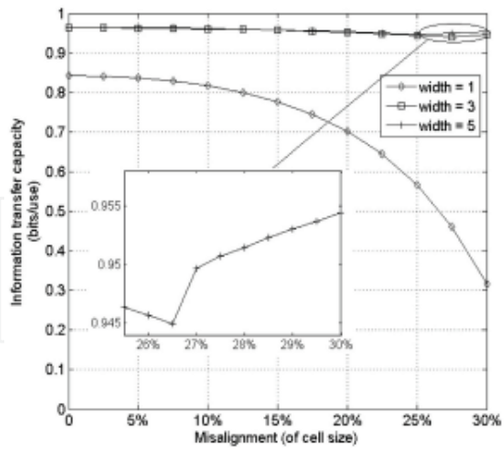

(a) QCA Line

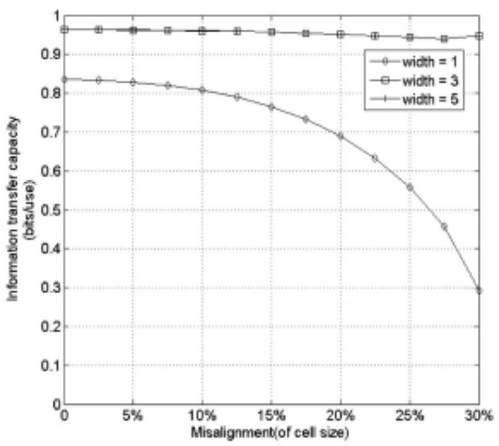

(b) QCA Inverter

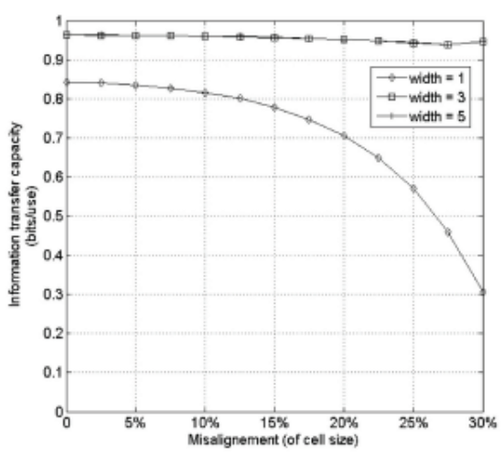

(c) QCA Majority

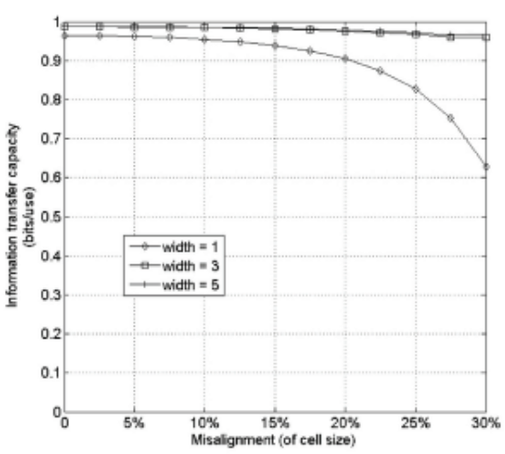

(d) QCA Crossbar

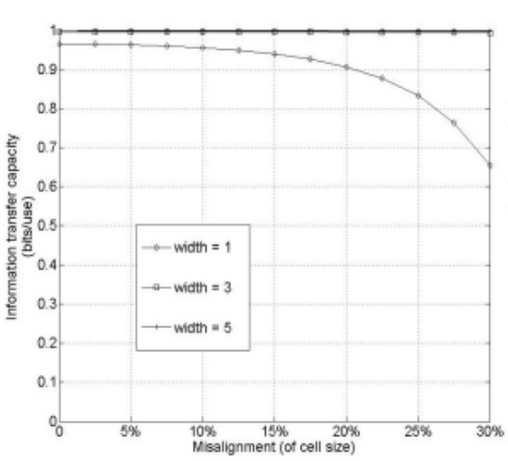

(e) QCA Fanout

Fig. 8. Information transfer capacity of QCA devices under cell misalignment defects.

QCA devices degrades quickly due to the probabilistic nature of their operation. This may be a significant issue for robust nanocomputing. Also, to achieve the same level of reliability, a higher level of spatial redundancy is needed if the displacement is large. For the example of the QCA line shown in Fig. 7(a) with a displacement of 30% of cell size, a width = 5 is needed to achieve an information transfer capacity of 0.69 bits/use (a width = 3 achieves the same information transfer capacity at a displacement of 27.5%). Finally, although tile-based design can improve the reliability of QCA devices, the effectiveness of this approach saturates quickly with an increase in width. This shows that it is difficult to further improve the reliability of QCA devices beyond a certain level of spatial redundancy. The simulated QCA devices are single output gates. Under the ideal (error- and variation-free) operation, the information transfer capacity will be equal to 1 bit/use while it will be less than 1 bit/use in the presence of defects and variations.

The effect of cell misalignment on the reliability of QCA devices has also been studied. A scenario of cell misalignment defects is shown in Fig. 6(b) for QCA lines; each pair of neighboring cells has the same offset d_f from the center line. This corresponds to the worst case scenario, e.g., the largest difference in kink energy (refer to (23) and (24)).

Figure 8 shows the information transfer capacity of QCA devices under cell misalignment defects ranging from 0% to 30% of cell size. The relationship of information transfer capacity, defects, and level of spatial redundancy follows a similar trend as for the QCA devices under cell displacement defects. Compared to the results in Fig. 7, the information transfer capacity of QCA devices under cell misalignment is larger than under cell displacement. This is consistent with the observation that QCA technology is relatively less sensitive to cell misalignment defects.

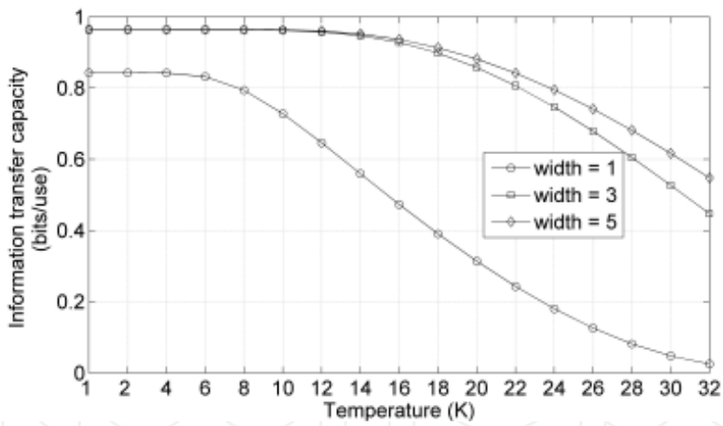

Fig. 9. Information transfer capacity of QCA lines under different temperatures.

Another interesting observation drawn from Fig. 8 is that for some QCA devices, the information transfer capacity does not monotonously decrease with an increase in misalignment among QCA cells. For example in Fig. 8(a), the information transfer capacity of the QCA line with a width of 5 increases slightly at a misalignment of 26.5% of cell size. This seems to counter the well-prevalent intuition; however, a careful examination of this result reveals that when the misalignment is nearly 26.5% of the cell size, the QCA line actually acts like a QCA inverter due to entanglement among misaligned QCA cells, i.e., the QCA line generates more flipped outputs. According to the discussion related to Fig. 2, the output can be interpreted by its complement to get more correct results. While the QCA function is fixed,

this interpretation is by default reflected in the information-theoretic measures (as shown in Fig. 2). From these results, we can see that the proposed information-theoretic analysis can effectively quantify the impact of various defects on reliable operation, e.g., cell displacement will reduce the reliability monotonically, while cell misalignment may cause a sudden change of device functionality.

Finally, we apply the proposed method to study the impact of temperature on QCA operation. Figure 9 shows the information transfer capacity of QCA lines implemented with different widths subject to variations in temperature from $1K$ to $32K$; QCA lines become less reliable for all implementations as temperature increases, but a high level of spatial redundancy utilization achieves a better reliability.

5. Conclusion

An information-theoretic framework has been developed for the analysis of stochastic behaviors in QCA devices. The proposed method establishes a direct correspondence between spatial redundancy and the reliability of this technology in the presence of defects and variations, thereby allowing to evaluate the capabilities and limitations of QCA-based nanocomputing systems. We have conducted a comprehensive set of simulations on different QCA devices. These results show that the proposed method can be used to address the evaluation of the reliability as achieved under a specified level of spatial redundancy; also the proposed method allows to quantitatively evaluate the uncertainties in the operation of QCA devices.

From an information-theoretic perspective, reliability measured by the information transfer capacity can be interpreted as an upper bound (of which the numerical values are determined by specific design techniques) that QCA devices can achieve. The proposed method does not specify a design technique that would achieve this bound because the proposed method is derived from (Shannon, 1948), i.e., to establish an achievable bound on the information transfer capacity but not the method for achieving such a bound. In the absence of a general theory, the method proposed in this paper focuses on determining the information transfer capacity. The ability to determine this achievable bound has substantial implications on the design optimization of QCA devices and circuits.

6. References

Lent, C. S., Tougaw, P. D., Porod, W. and Bernstein, G. H. (1993). Quantum cellular automata, *Nanotechnology*, pp.49-57, vol. 4.

Lent, C. S. and Tougaw, P. D. (1997). A device architecture for computing with quantum dots, *Proceeding of the IEEE*, 541-557.

Amlani, I., Orlov, A., Snider, G. and Lent, C. (1998). Demonstration of a functional. quantum-dot cellular automata cell, *J. Vac. Sci. Tech. B.*, vol. 16, 3795-3799.

Cowburn, R. and Welland, M. (2000). Room temperature Magnetic Quantum Cellular Automata, *Science*, 1466-1468.

Smith, C., Gardelis, S., Rushforth, A., Crook, R., Cooper, J., Ritchie, D., Lineld, E., Jin, Y. and Pepper, M. (2003). Realization of quantum-dot cellular automata using semiconductor quantum dots, *Super lattices and Microstructures*, vol. 34, 195-203.

Jiao, J., Long, G., Grandjean, F., Beatty, A. and Fehlner, T. (2003). Building blocks for the molecular expression of Quantum Cellular Automata. Isolation and characterization

of a covalently bonded square array of two ferrocenium and two ferrocene complexes, *J. Am. Chem. Soc.*, vol. 125, 1522-1523.

Momenzadeh, M., Huang, J. and Lombardi, F. (2005). Defect characterization and tolerance of QCA sequential devices and circuits, *Defect and Fault Tolerance in VLSI Systems*, 199-207.

Tahoori, M. B., Momenzadeh, M., Huang, J. and Lombardi, F. (2004). Defects and faults in quantum cellular automata at nano scale, *VLSI Test Symposium*, 291-296.

Niemier, M., Crocker, M., Hu, X. S. and Lieberman, M. (2006). Using CAD to shape experiments in molecular QCA, *Int. Conf. on Comp. Aided Design*, 907-914.

Ottavi, M., Pontarelli, S., Vankamamidi, V., Salsano, A. and Lombardi, F. (2006). QCA memory with parallel read/serial write: design and analysis, *IEE proceeding circuit, devices, and systems*, vol. 153, 199-206.

Frost, S., Rodrigues, A. F., Janiszewski, A. W., Raush, R. T. and Kogge, P. M. (2002). Memory in motion: A study of storage structures in QCA, *First Workshop on Non-Silicon Computing*.

Vankamamidi, V., Ottavi, M. and Lombardi, F. (2005). Tile Based Design of a Serial Memory in QCA, *Proceedings of ACM Great Lakes Symposium on VLSI*, 201-206.

Niemier, M. T. and Kogge, P. M. (1999). Logic in wire: using quantum dots to implement a microprocessor, *IEE proceeding circuit, devices, and systems*, 118-121.

Dutta, M. and Stroscio, M. A. (2000). Quantum-based electronic devices and systems, *World scientific publishing company*.

Niemier, M. T. (2004). Designing digital systems in quantum cellular automata, *Master's thesis, University of Notre Dame*.

Walus, K. and Jullien, G. A. (2006). Design tools for an emerging SoC technology: quantum-dot cellular automata, *Proceedings of IEEE*, vol. 94, 1225-1244.

Tougaw, P. D. and Lent, C. S. (1994). Logical devices implemented using quantum cellular-automata, *Journal of Applied Physics*, vol. 75, 1818-1825.

Wei, T., Wu, K., Karri, R. and Orailoglu, A. (2005). Fault tolerant quantum cellular array (QCA) design using Triple Modular Redundancy with shifted operands, *2005 conference on Asia South Pacific design automation* , 1192-1195.

Fijany, A. and Toomarian, B. N. (2001). New design for quantum dots celluar automata to obtain fault tolerant logic gates, *Journal of Nanoparticle Research*, 27-37.

Huang, J., Momenzadeh, M. and Lombardi, F. (2006). On the tolerance to manufacturing defects in molecular QCA tiles for processing-by-wire, *Journal of Electronic Testing: Theory and Applications*, 163-174.

Huang, J., Momenzadeh, M. and Lombardi, F. (2006). Defect tolerance of QCA tiles, *Design, Automation and Test in Europe*, 1-6.

Dysart, T. J. (2005). Defect properties and design tools for quantum dot cellular automata, *Master's thesis, University of Notre Dame*.

Liu, M. (2006). Robustness and power dissipation in quantum-dot cellular automata, *Ph.D. Dissertation, University of Notre Dame*.

Ungarelli, C., Francaviglia, S., Macucci, M. and Iannaconne, G. (2000). Thermal behavior of quantum cellular automaton wires, *J. Appl. Phys.*, 7320-7325.

Wang, Y. and Lieberman, M. (2004). Thermodynamic behavior of molecular-scale quantum-dot automata (QCA) wires and logic devices, *IEEE Trans. on Nano.*, 368-376.

Dysart, T. J. and Kogge, P. M. (2007). Probabilistic analysis of a molecular quantum-dot cellular automata adder, *IEEE International Symposium on Defect and Fault Tolerance in VLSI Systems*, 478-486.

Bhanja, S., Ottavi, M., Lombardi, F. and Pontarelli, S. (2006). Novel designs for thermally robust coplanar crossing in QCA, *Design Automation and Test in Europe*, 786-791.

Bhanja, S. and Sarkar, S. (2006). Probabilistic modeling of QCA circuits using bayesian networks, *IEEE Transactions on Nanotechnology*, 657-670.

Srivastava, S. and Bhanja, S. (2007). Hierarchical probabilistic macromodeling for QCA circuits, *IEEE Transactions on Computers*, 174-190.

von Neumann, J. (1955). Probabilistic logics and the synthesis of reliable organisms from unreliable components, *Automata Studies, Shannon C.E.and McCarthy J., eds.*, Princeton University Press, Princeton N.J., pp. 43-98.

Pippenger, N. (1985). On networks of noisy gates, *Proc. 26th Annu. Symp. on Foundations Comput. Sci.*, pp. 30-36.

Pippenger, N. (1989). Invariance of complexity measures for networks with unreliable gates, *Journal of the ACM.*, vol. 36, pp. 531-539.

Hajek, B. and Weller, T. (1991). On the maximum tolerable noise for reliable computation by formulas, *IEEE Trans. Inf. Theory*, vol. 37, no. 2, pp. 388-391.

Evans, W. and Schulman, L. J. (1999). Signal propagation and noisy circuits, *IEEE Trans. Inf. Theory*, vol. 45, no. 7, pp. 2367-2373.

Evans, W. and Pippenger, N. (1998). On the maximum tolerable noise for reliable computation by formulas, *IEEE Trans. Inf. Theory*, vol. 44, no. 3, pp. 1299-1305.

Gao, J. B., Qi, L., and Fortes, J. A. B. (2005). Bifurcations and fundamental error bounds for fault-tolerant computations, *IEEE Trans. on Nanotechnology*, pp. 395-402.

Bhaduri, D. and Shukla, S. (2005). NANOLAB – A tool for evaluating reliability of defect-tolerant nanoarchitectures, *IEEE Trans. on Nanotechnology*, vol. 4, pp. 381-394.

Sotiriadis, P. P. (2006). Information capacity of nanowire crossbar switching networks, *IEEE Trans. on Information Theory*, vol. 52, pp. 3019- 3032.

Wang, L. and Shanbhag, N. (2003). Energy-efficiency bounds for deep submicron VLSI systems in the presence of noise, *IEEE Transactions on VLSI Systems*, vol. 11, 254-269.

Dai, J., Wang, L. and Jain, F. (2009). Analysis of defect tolerance in molecular crossbar electronics, *IEEE Transactions on VLSI Systems*, vol. 17, 529-540.

Shannon, C. E. (1948). A mathematical theory of communication, *Bell Syst. Tech. J.*, vol. 27, part I, 379-423, part II, 623-656.

Timler, J. and Lent, C. S. (2002). Power gain and dissipation in quantum-dot cellular automata, *Journal of applied physics*, vol. 91, 823-831.

Timler, J. and Lent, C. S. (1996). Dynamic behavior of quantum cellular automata, *Joural of applied physics*, vol. 80, 4722-4736.

Mahler, G. and Weberruss, V. A. (1998). Quantum networks: dynamics of open nanostructures, *New York: Springer-Verlag*.

Hennessy K. and Lent, C. S. (2001). Clocking of molecular quantum-dot cellular automata, *Journal of Vacuum Science and Technology*, 1752-1755.

Niemier, M., Alam, M., Hu, X. S., Bernstein, G., Porod, W., Putney, M. and DeAngelis, J. (2007). Clocking structures and power analysis for nanomagnet-based logic devices, *Proc. of international symposium on Low power electronics and design* , 26-31.

Walus, K., Dysart, T. J., Jullien, G. A. and Budiman, R. A. (2004). QCADesigner: a rapid design and simulation tool for quantum-dot cellular automata, *IEEE transcation on Nanotechnology*, 26-29.

Schulhof, G., Walus, K. and Jullien, G. A. (2007). Simulation of random cell displacements in QCA, *ACM Journal on Emerging Technologies in Computing Systems*, Vol. 3, Issue 1, Artical No. 2.

Cellular Automata - Innovative Modelling for Science and Engineering

Edited by Dr. Alejandro Salcido

ISBN 978-953-307-172-5
Hard cover, 426 pages
Publisher InTech
Published online 11, April, 2011
Published in print edition April, 2011

Modelling and simulation are disciplines of major importance for science and engineering. There is no science without models, and simulation has nowadays become a very useful tool, sometimes unavoidable, for development of both science and engineering. The main attractive feature of cellular automata is that, in spite of their conceptual simplicity which allows an easiness of implementation for computer simulation, as a detailed and complete mathematical analysis in principle, they are able to exhibit a wide variety of amazingly complex behaviour. This feature of cellular automata has attracted the researchers' attention from a wide variety of divergent fields of the exact disciplines of science and engineering, but also of the social sciences, and sometimes beyond. The collective complex behaviour of numerous systems, which emerge from the interaction of a multitude of simple individuals, is being conveniently modelled and simulated with cellular automata for very different purposes. In this book, a number of innovative applications of cellular automata models in the fields of Quantum Computing, Materials Science, Cryptography and Coding, and Robotics and Image Processing are presented.

InTech Europe
University Campus STeP Ri
Slavka Krautzeka 83/A
51000 Rijeka, Croatia
Phone: +385 (51) 770 447
Fax: +385 (51) 686 166
www.intechopen.com

InTech China
Unit 405, Office Block, Hotel Equatorial Shanghai
No.65, Yan An Road (West), Shanghai, 200040, China
中国上海市延安西路65号上海国际贵都大饭店办公楼405单元
Phone: +86-21-62489820
Fax: +86-21-62489821

IntechOpen